Directional Warhead Design Methodology for a Tailored Fragment Beam

Kusumkant D. DHOTE [1,*], Krothapalli P. S. MURTHY [1],
Kizhakkel M. RAJAN [1], Mahesh M. SUCHEENDRAN [2]

[1] *Armament Research & Development Establishment, Armament*
  Post, Dr. Homi Bhabha Road, Pashan, Pune – 411021, India
[2] *Defence Institute of Advanced Technology,*
  Girinagar, Pune – 411025, India
*E-mail: kddhote@gmail.com

Abstract: In this article, the authors present a design methodology for generating a spatially tailored fragment beam with specified velocity and projection angles. The modified Gurney equation was used to estimate the length and diameter of the cylindrical charge to achieve the desired velocity; and the modified Taylor equation was used to arrive at the radius of curvature of the fragmenting disc. The methodology is further explained for generating a rectangular beam of fragments having a velocity of 1500 m/s with a tailored fragment beam of 32° in the azimuth and 20° in the elevation. The warhead had preformed steel fragments of 4 mm diameter arranged in a double layer. The design was validated using the fragment distribution measured experimentally.

Keywords: Gurney equation, Taylor equation, coherent fragment distribution, high explosive, arena test setup

1 Introduction

Directional fragmentation warheads are often deployed for neutralizing the tactical ballistic missile class of targets. These warheads are designed with a spatially tailored fragment beam, focussed towards the target to enhance the lethality. A warhead having preformed fragments is a better choice because it gives better lethality than natural fragmentation. Conventional warheads have

a uniform fragment beam around the axis, with only 5 to 10 percent of the total fragments projecting onto the areal target, the remaining ones being unutilized [1]. This limitation can be overcome with a directional fragment generator warhead (FGW). On explosion, it projects around 50 percent of the fragments in a coherent conical beam towards the target. These fragments originate from the central region of the fragmenting disc, which is approximately 0.7 times the explosive charge radius [2]. However, the fragmenting disc needs to be oriented towards the target before it is fired.

The conventional design of FGW has a circular fragmenting disc [2, 3]. The spatial distribution of the fragments mainly depends on the contours of the fragmenting disc. Concave and convex shaped profiles give concentrated and dispersed fragments sprayed in a cone, respectively. The warhead parameters which significantly determine the fragment spatial distribution are the mass ratio of the explosive charge to the fragmenting metal disc (C/M), the ratio of the length to diameter (L/D) of the explosive charge, and the explosive characteristics. The spatial distribution is quantified using the fragment velocity and the projection angle, which is estimated using the Gurney [4] and Taylor [5] equations, respectively. These equations are derived considering infinite geometries in two directions of the Cartesian coordinates, which simplifies the problem to a one dimensional problem. Although they are good engineering approximations, estimates using these equations for a warhead with finite dimensions result in significant deviations in the predictions of spatial distribution due to lateral effects and energy losses [6]. This has been taken care of by modifying the Gurney equation by incorporating the L/D ratio [7]. The Taylor equation has also been modified by incorporating the effects of the detonation front interaction direction and the shape of the fragmenting disc [8].

The fragment spatial distribution of FGW has been studied for an axi-symmetric circular fragmenting disc by a few researchers [2, 3, 7]. Depending on the specific weapon deployment conditions, it may be necessary to have a tailored fragment distribution in a square-, rectangular- or oval-shaped spray pattern. The spatial distribution of fragments from a square-shaped fragmenting disc was studied by Held [9].

The authors present a methodology for designing a directional FGW generating a rectangular fragment beam. This is explained for the objective of creating a rectangular fragment beam of cone angle 32° by 20°, with a fragment velocity of the order of 1500 m/s using 4 mm diameter spherical steel fragments arranged in two layers. The modified Gurney and Taylor equations were used to decide the contours of the fragmenting surface. The designed warhead was tested and the results are discussed.

2   Design Methodology

For a given explosive, the key parameters governing the fragment velocity are the mass ratio of the explosive charge to the fragmenting metal disc (C/M) and the length to diameter ratio (L/D) of the explosive charge. In the case of a cylindrical charge having a fragmenting disc at one end of the cylinder with initiation at the other end, the modified Gurney equation was used to calculate the fragment velocity [7]. A parametric study to investigate the effect of the C/M and L/D ratios on the fragment velocity was carried out for the HMX/TNT (70/30) high explosive having a Gurney characteristic velocity, $\sqrt{(2E)}$, of 2800 m/s. The fragment velocities for a range of C/Ms were estimated for different L/Ds using Equation 1. A velocity correction factor 'c' of 0.9 was considered [3]. The estimates are plotted in Figure 1.

$$V = c \cdot \sqrt{2E} \, \frac{\sqrt{3}\left(\frac{C}{M}\right)}{\left\{\left(\frac{C}{M}+4\right)\left(\frac{C}{M}+1\right)\left(1+2\frac{L}{D}\right)\right\}^{\frac{1}{2}}} \qquad (1)$$
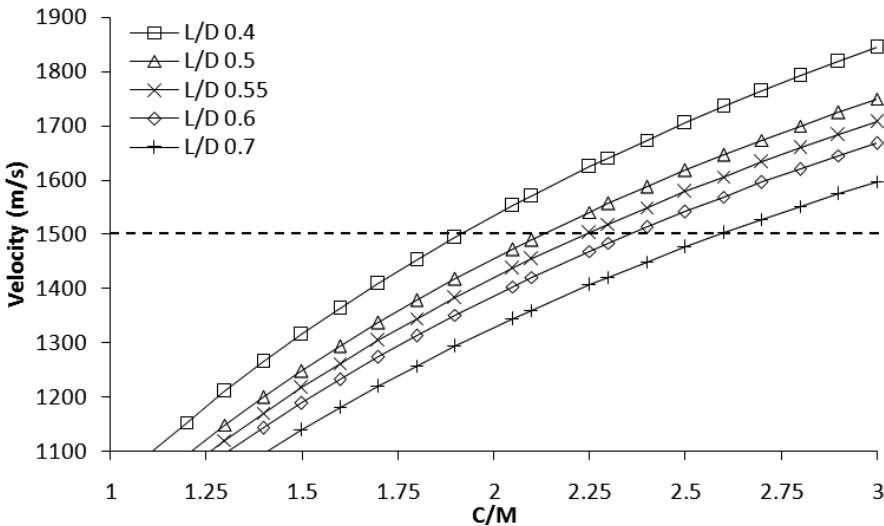

Figure 1.   Variation of the fragment projection velocities with the C/M and L/D ratios.

From the Figure 1, it is observed that for a given C/M ratio, a low L/D ratio yields a higher fragment velocity. Further, at lower C/M the effect of L/D on the change in velocity is less than at higher C/M. Furthermore, for a given L/D, the

slope of the line showing change in fragment velocity at various C/M ratios is higher at lower C/M ratios. The possible combinations of L/D and C/M ratios that yield fragment velocities around 1500 m/s are given in Table 1.

Table 1.   FGW details for 4 mm steel spherical fragments in two layers

L/D	C/M	D	L	N	W	H	C	M_{km}
0.70	2.60	77	54	643	54	87	445	643
0.60	2.35	82	49	715	57	92	448	667
0.55	2.25	86	47	781	60	96	468	707
0.50	2.15	90	45	862	63	101	494	758
0.40	1.90	107	43	1225	75	120	669	1044

L/D: Explosive length to diameter ratio; C/M: Explosive charge to metal mass ratio; D: Explosive charge diameter in mm; L: Explosive charge length in mm; N: Total number of fragments; W: Explosive width in mm; H: Explosive height in mm; C: Explosive charge mass in g; M_{km}: Kill mechanism mass in g.

The C/M ratio for multiple layers of fragments in a cylindrical configuration of FGW was estimated using Equation 2. The explosive charge mass (C) was estimated from the cross sectional area of the cylinder (a_D), the length of the explosive column (L) and the explosive density (ρ_f). The fragmenting metal disc was assumed to have an area equal to the cross sectional area of the charge (a_D) and the fragments were laid on it, using a resin mix. Its mass (M) was estimated from the number of fragment layers (n_l), the mass of each fragment (m_f), a factor for the packing of fragments on the disc (f_p) and the number of fragments. The number of fragments was considered as the ratio of the area of the fragmenting disc (a_D) and the area of each fragment (a_f). For an estimate of the C/M ratio, the proportionate mass of the disc and resin mix was included in the fragment mass (m_f). Rearranging Equation 2, one obtains Equations 3 and 4 for the estimation of the explosive charge length (L) and diameter (D), respectively.

$$\frac{C}{M} = \frac{a_D L \rho_e}{n_l m_f f_p \frac{a_D}{a_f}} \tag{2}$$

$$L = \frac{C}{M} \frac{n_l m_f f_p}{\rho_e \, a_f} \tag{3}$$

$$D = \left\{ \frac{C/M}{L/D} \right\} \frac{n_l \, m_f f_p}{\rho_e \, a_f} \tag{4}$$

The fragment size may be decided based on the desired lethality, defined in terms of the fragment hit density and its penetration capability at the desired range on the specified target. However, for the sake of explaining the design methodology, a spherical steel fragment of diameter 4 mm and having a mass of 0.261 g was chosen. The fragments were arranged in two layers on the disc. Furthermore, the design of the FGW was proposed to yield a rectangular, symmetric coherent fragment beam of 32° by 20°, with an overall mass of kill mechanism close to 700 g.

The mass of 5 mg/fragment was assumed for the resin mix and the disc on which the fragments were arranged. Hence, the mass of each fragment was 0.266 g. The factor for packing (f_p) of the spherical fragments on the disc was considered to be 0.85. The number of layers (n_l) on the disc was two and the explosive density (ρ_e) was 1.72 g/cm³. The calculated FGW parameters for various combinations of L/D and C/M are given in Table 1. The estimated circular fragmenting disc area was converted to a proportionate height (H) and width (W) of the rectangular fragmenting disc area, which was calculated from the ratio of the required projection angles 32° to 20°. The estimated H/W was 1.6. Table 1 also gives values for the explosive charge mass and mass of kill mechanism (M_{km}), which includes the total mass of fragments, explosive, disc and resin mix. The combinations of L/D and C/M need to be adjusted for deciding the design parameters based on the overall space, mass and lethality constraints.

To keep the mass of kill mechanism around 700 g, a design having L/D of 0.55 and C/M of 2.25 is given in Table 1, and was chosen for experimental evaluation. Since the C/M ratio was very high, the spall mitigation technique as discussed by Dhote *et al*. [11] was adopted in the design.

A conventional cylindrical FGW having a flat circular fragmenting disc results in a conically divergent coherent beam of around 15° [2]. A fragment beam of 32° by 20° can be achieved with a rectangular convex fragmenting disc. For ease of manufacture, the shape of the convex fragmenting disc was chosen to be of spherical curvature.

On detonation of a spherical charge at the centre, the detonation wave interacts in a normal direction throughout the fragmenting surface. Hence, it expands uniformly and sprays the fragments in a direction normal to the surface. However, when the spherical charge is not initiated at the centre, the incidence of the detonation front is not normal to the fragmenting surface. Hence, there will be a deviation in the projection angle of fragments. In such cases, the projection angle is estimated with modified Taylor equations [8]. The deviation in the projection angle about the normal to the fragmenting surface (θ) is estimated using Equation 5. The angle between the normal to the fragmenting surface and

the warhead axis is $\emptyset_1$. The angle between a line joining the explosive initiation point to the fragmenting surface and the warhead axis is $\emptyset_2$. The angles are shown in the Figure 2.

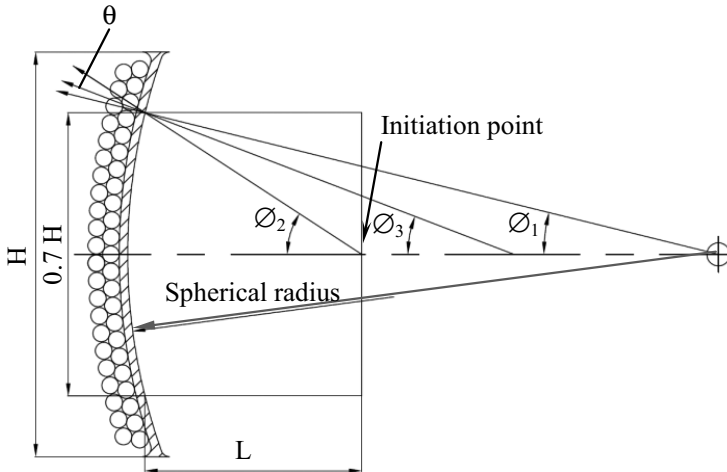$$\theta = \left| tan^{-1} \left[\left(\frac{V_0}{2U} \right) \cos \left(\frac{\pi}{2} + \emptyset_2 - \emptyset_1 \right) \right] \right| \qquad (5)$$

Figure 2. Projection angles.

The radius of the fragmenting disc was selected based on the deviation in the projection angle. From the experimental results for various geometries of the fragmenting disc by Dhote *et al.* [2], it was observed that the fragments originating from the central area, of 0.7 times the radial distance, form a coherent beam, and the remaining fragments had large deviations due to edge effects. Hence, fragments within 0.7 times the height and width of the fragmenting disc were expected in the beam. The height and width of the scaled down warhead were 96 and 60 mm, respectively. 0.7 times the height and width worked out to be 67.2 and 42 mm, respectively. It was expected that the fragments in the central region of 67.2 by 42 mm of the fragmenting disc would form a coherent beam. For various radii of the fragmenting disc, the projection angle $(\emptyset_3)$ was estimated using Equation 6 and is given in Table 2 for a length of explosive column (L) of 47 mm. The velocity of detonation (U) for the explosive was 8300 m/s. It was observed that a spherical radius of 140 mm meets the fragment beam in both directions. The azimuth and elevation directions given in Table 2 correspond to the height of 96 mm and width of 60 mm, respectively.

$$\emptyset_3 = \theta + \emptyset_1 \tag{6}$$

Table 2.   Effect of the spherical radius on the projection angle

R	Azimuth				Elevation			
	$\emptyset_1$	$\emptyset_2$	θ	$\emptyset_3$	$\emptyset_1$	$\emptyset_2$	θ	$\emptyset_3$
130	14.98	35.56	1.82	16.80	9.30	24.08	1.32	10.62
140	13.89	35.56	1.91	15.80	8.63	24.08	1.38	10.01
150	12.94	35.56	1.99	14.93	8.05	24.08	1.43	9.48

R: Sphere radius in mm; $\emptyset_1$: Angle between normal to surface and warhead axis in degrees; $\emptyset_2$: Angle between direction of detonation and warhead axis in degrees; θ: Deviation angle from normal to the surface in degrees; $\emptyset_3$: Projection angle in degrees.
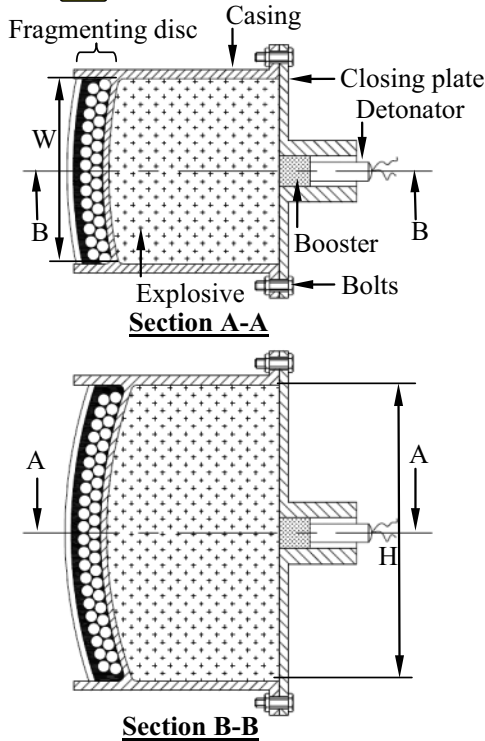
3 Experimental

Figure 3.   Warhead configuration.

The warhead casing was made of aluminum alloy, giving 3 mm thick confinement all around the explosive. A schematic diagram of the FGW subjected to experimental testing is shown in Figure 3. The fragmenting disc was made as a part of the casing, which had 2 mm thickness and an inner radius of 140 mm. The disc surface was covered with 4 mm steel spheres in two layers, using a resin mixed with iron powder. A spall mitigating layer of 2 mm thick resin mixed with iron powder and 2 mm thick aluminum alloy sheet was provided on the outer surface of the fragments. The high explosive HMX/TNT (70/30) was filled into the casing and the closing plate was integrated using bolts. A RDX/wax (95/5) booster having a diameter of 10 mm and length of 10 mm was inserted in the closing plate. An electrical detonator was used for initiation of the booster. Two tests with similar configurations were carried out.

The arena test setup for the experiment to assess the spatial distribution of the fragments and their initial velocities is shown in Figure 4. The warhead was placed at a height of 1.2 m on a wooden stand. The steel target plates were 1.5 mm thick, of height 2.4 m and width 1.2 m. The target plates were placed at a distance of 5 m from the warhead. The target plate covered a 27° cone angle in elevation. Six target plates were placed to cover fragment spatial distribution, covering 7.2 m in the azimuth direction with a 70° cone angle. The target plates were marked in 2° intervals in the azimuth and elevation directions to record the fragment spatial distribution. The warhead was aligned to the centre of the target. The warhead width (W) corresponds to the elevation and its height (H) corresponds to the azimuth of the target. Multi-channel electronic counters were placed in front of the target plates to record the initial fragment velocities. The fragment velocities were estimated from the distance and time records.
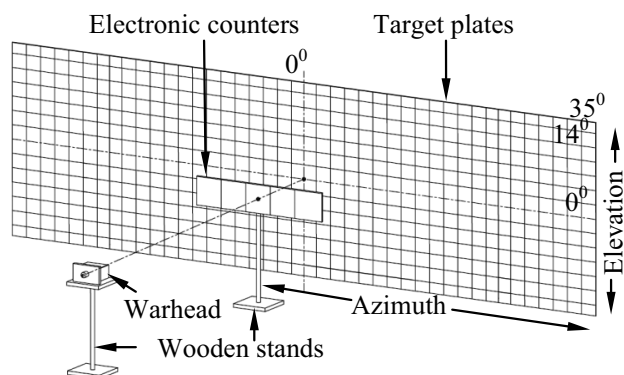

Figure 4. Arena test setup for the experiments.

4   Results and Discussion

Variations in the two test results were expected due to randomness in the manual fragment laying process, in the casing expansion process, in the fracture process of the fragmenting surface and gas leakages through it, and in the inter-layer fragment interactions before their separation. For analysis purposes, the data were averaged for the two experiments. The average spatial distribution of the fragments is shown in Figure 5. Since, the warhead had planar symmetry in the elevation and azimuth directions, the number of fragments recorded in the marking of the 2° by 2° cone was merged and the average data were plotted in a three dimensional graph, representing the first quadrant of the target.
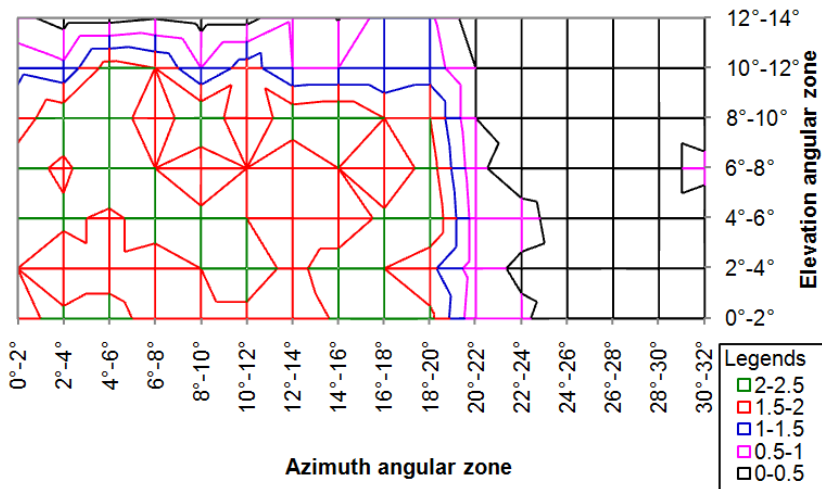

Figure 5. Fragment spatial distribution in the azimuth for the entire data.

In Figure 5, the colour code shows the range of fragments. The intersection points of horizontal and vertical lines represents the number of fragment in the respective 2° by 2° cones. It was observed that in the desired fragment beam of 32° (± 16°) by 20° (± 10°), the number of fragments was in the range of 1.5 to 2.5 and the fragment beam was coherent. The percentage of fragments in this range was 42. The average hit density distributions in this region, in the azimuth and elevation directions, are shown in Figure 6 and 7, respectively. This also indicates that the hit density is around 62 fragment hits/m² in the designed beam for the FGW.
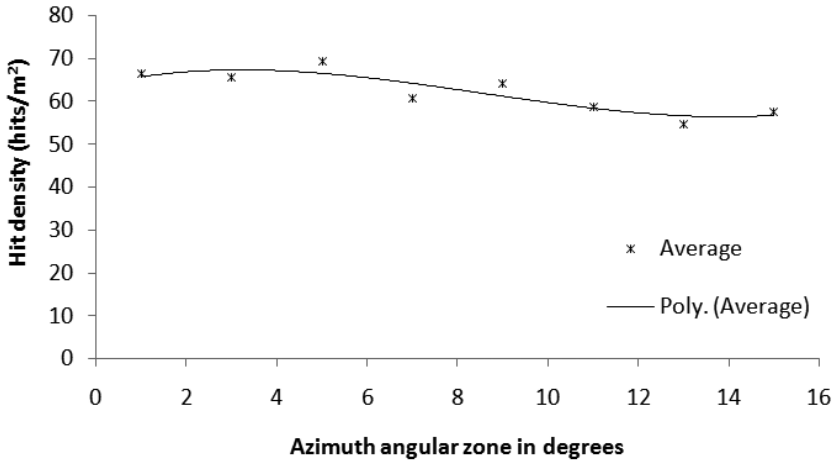
Figure 6. Fragment hit density on the target at 5 m in the azimuth direction.
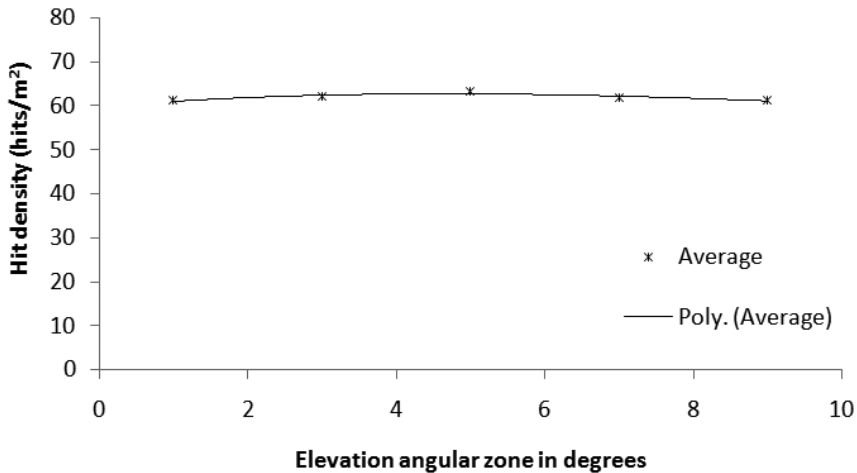

Figure 7.   Fragment hit density on the target at 5 m in the elevation direction.

The warhead was designed to have a fragment velocity of 1500 m/s. The equation for a cylindrical configuration of the FGW was used for the estimation of the velocity, and the cylindrical area was configured to a rectangular beam proportional to the fragment beam requirements. The recorded fragment velocities in the experiments were in the range of 1407 to 1581 m/s, which was in the range for the designed FGW.

From Figure 5, it was also observed that the coherent fragment beam of 1.5

to 2.5 fragments was around 40° (± 20°) degrees in azimuth and 24° (± 12°) in elevation. The percentage of fragments in this beam was 59. Compared to the expected fragment beam of 32° in azimuth and 20° in elevation, 8° and 4° more beam was observed in the experiment, respectively. In the designed warhead, the velocity variation from the central fragments to the fragments on the edge of the fragmenting surface was not considered. Due to the spherical fragmenting disc, the central fragments had the highest C/M ratios and the fragments on edge had the lowest C/M ratios. As a result, the central fragments gained the highest velocity and for the remaining fragments the velocity decreased gradually towards the edge. This velocity variation from centre to edge contributed to the increase in the projection angle in radial directions. Further, the deviation in the fragment projection angle contributed by dispersion quantification as a normal distribution with a standard deviation of 0.75° [2]. Yet another contributing factor for the increased fragment beam was the multilayer fragment interactions before becomes separated.

Beyond around 40° (± 20°) in azimuth and 24° (± 12°) in elevation, the edge effects were dominant. The fragment spray becomes dispersed and fewer fragments impact on the target. Still, in azimuth between 40° (± 20°) and 48° (± 24°) and in elevation between 24° (± 12°) and 28° (± 14°), the number of fragment varied between 0.5 and 1.5. The percentage of fragments between 48° (± 24°) in azimuth and 28° (± 14°) in elevation was 66. Between 64° (± 32°) and 48° (± 24°) in the azimuth direction, the number of fragments was less than 0.5, and beyond 64° (± 32°) up to 70° (± 35°) there were no fragments at all. The total percentage of fragments recovered on the target was 69%. The remaining fragments were expected to have higher projection angles than the target coverage and most of them in elevation could not have impacted on the target.

59% of the fragments were in the coherent beam, which is 0.76 times the width and height of the fragmenting surface. These observations were similar to those in [2], where the coherent beam of fragments was generated through a central region of around 0.7 times the radius of the fragmenting disc. The remaining fragments were deviated due to edge effects.

5   Conclusions

The design methodology for FGW using modified Gurney and Taylor equations has been explained for the generation of a fragment beam of 32° in azimuth and 20° in elevation, with fragment velocities of 1500 m/s for two layered steel fragments having a diameter of 4 mm. The modified Gurney equation was used to

estimate the cylindrical explosive charge diameter and length. The five different combinations of L/D and C/M, which give a fragment velocity of 1500 m/s were (0.70, 2.60), (0.60, 2.35), (0.55, 2.25), (0.50, 2.15) and (0.40, 1.90). Maintaining an explosive length at 47 mm, a height of 96 mm and width of 60 mm, was estimated for a beam of aspect ratio 1.6, which is based on a mass restriction of 700 g and an average number of fragments greater than or equal to 1.5 in each angular zone of 2° by 2°. Using the modified Taylor equation, a 140 mm radius of curvature for the fragmenting disc surface was selected based on an estimated half cone projection angle of 15.80° in the azimuth and 10.01° in the elevation directions. The design methodology for the FGW was validated by conducting an arena test. It was observed that 59% of the fragments were in the coherent beam of 40° in azimuth and 24° in elevation, and the fragments from the central region, of 0.76 times the width and height, were in the coherent beam. The remaining fragments had deviated due to edge effects. A coherent beam larger than the designed one was attributed to variations in the effective C/M ratios from the central fragments to fragments on the edge of the FGW, dispersion in the projection angle and multilayer effects. The presented methodology would be useful for designing tailor made FGWs.

6   References

[1] Lloyd R.M., Physics of Direct Hit and Near Miss Warhead Technologies, in: *Progress in Astronautics & Aeronautics*, Vol. 194, (Zarchan P., Ed.), American Institute of Aeronautics and Astronautics, USA, **2001**, p. 6; ISBN 1-56347-473-5.

[2] Dhote K.D., Murthy K.P.S., Rajan K.M., Sucheendran M.M., Quantification of Projection Angle in Fragment Generator Warhead, *Defence Technology*, **2014**, *10*, 177-183.

[3] Qian L., Qu M., Wen Yu, Zhu Y., Jiang D., Dense Fragment Generator, *Propellants Explos. Pyrotech.*, **2002**, *27*, 267-278.

[4] Gurney R.W., *The Initial Velocities of Fragments from Bombs, Shells and Grenades*, BRL Report No. 405, Aberdeen Proving Ground, Maryland, USA, **1943**.

[5] Taylor G.I., Analysis of the Explosion of Long Cylindrical Bomb Detonated at One End, in: *The Scientific Papers of G. I. Taylor*, Vol. III (Batchelor G.K., Ed.), Cambridge at the University Press, UK, **1963**, pp. 277-286.

[6] Zlatkis A., Korin N., Gofman E., Edge Effects on Fragments Dispersion, *23rd Int. Symposium on Ballistics*, Tarragona, Spain, April 16-20, **2007**.

[7] Lloyd R.M., Physics of Direct Hit and Near Miss Warhead Technologies, in: *Progress in Astronautics & Aeronautics*, Vol. 194, (Zarchan P., Ed.), American Institute of Aeronautics and Astronautics, USA, **2001**, p. 250; ISBN 1-56347-473-5.

[8] Lloyd R.M., Conventional Warhead Physics, in: *Progress in Astronautics and*

Aeronautics, Vol. 179, (Zarchan P., Ed.), American Institute of Aeronautics and Astronautics, USA, **1998**, p. 374; ISBN 1-56347-255-4.

[9] Held M., Fragment Generator, *Propellants Explos. Pyrotech.*, **1988**, *13*, 135-143.

[10] Cooper P.W., *Explosive Engineering*, Wiley-VCH, New York, USA,**1996**, pp. 371-382; ISBN 0-471-18636-8.

[11] Dhote K.D., Verma P.N., Murthy K.P.S., Mitigation of Fragment Spall Induced by Explosive Loading in High Performance Fragment Generators, *Journal of Battlefield Technology*, **2014**, *17*(1).